NATIONAL UNIVERSITY OF SCIENCE AND TECHNOLOGY POLITEHNICA BUCHAREST

BRNO UNIVERSITY OF TECHNOLOGY

Doctoral School of Electronics, Telecommunications and Information Technology

Decision No. XXX **from** DD-MM-YYYY

Ph.D. THESIS SUMMARY

Ekaterina Svertoka

ÎMBUNĂTĂȚIREA PRECIZIEI DE LOCALIZARE A DISPOZITIVELOR PORTABILE INDUSTRIALE CU LORAWAN

ENHANCING LOCALIZATION ACCURACY IN INDUSTRIAL WEARABLES WITH LORAWAN

THESIS COMMITTEE

Prof. Mihai Ciuc, PhD UNSTPB	President
Prof. Ion Marghescu, PhD UNSTPB	PhD Supervisor
Assoc. Prof. Radim Burget, PhD Brno University of Technology	PhD Supervisor
Prof. Simona Lohan, PhD University of Tampere	Reviewer
Assoc. Prof., Angela Digulescu-Popescu, PhD Military Technical Academy (MTA) Ferdinand I	Reviewer
Assoc. Prof. Jiry Hosek, PhD Brno University of Technology	Reviewer
Assoc. Prof., Alexandru Martian, PhD UNSTPB	Reviewer

BUCHAREST 2024

Table of contents

Chapter 1

Introduction

1.1 Motivation

At the start of this research work in 2019, the number of people who had been injured or had died in the workplace was estimated in the millions [1], and the decrease in victims in the next two years was explained more by a serious reduction or closure of production facilities during the pandemic rather than by improved working conditions or an increase in workplace safety measures. The global research field of this work, industrial wearable devices for ensuring work safety, arose to deal with this problem and is based on indifference and the desire to improve the world.

The increase of the safety level in industries, hazardous factories, and simple organizations is a long-term process, profoundly affecting the structure of the work processes in a company. Nowadays, this process could be supported and significantly accelerated by modern technologies provided within Industry 4.0. The core part of the modification and digitalization of the industries gained the concept of the Internet of Things (IoT) and one of its main directions – wearable technology.

In this work, we first explored state-the-art industrial wearables for work safety. Among the various methods of contributing to the topic, we focused on a cluster of localization-related unsolved problems, considering it one of the most important and expansive fields for research in the area. The combination of the theoretical and practical research tracks led us to investigate the possibility of using LoRaWAN to localize wearables in dangerous workplace applications. At that time, this area was poorly studied for a complex reason: LoRaWAN was not initially designed for localization purposes and had limitations in the form of a small bandwidth, which hints at low accuracy from the beginning. On the other side, several features would be attractive for localization performed by *low-power* IIoT devices, thus, it is feasible to increase precision using additional preprocessing or postprocessing methods and save energy. This way, society may receive a low-cost, low-power, wide-range solution that would guarantee sufficient positioning accuracy for wearables, especially for work safety scenarios.

1.2 Research problems and contribution

The thesis puts in spotlight 3 Research Questions (RQ), each to be followed with the specific type of contribution, shown in Table 1.1.

Table 1.1 Main research contributions

№	Research question	Contribution type
RQ1	Investigation of the metrics and functions of wearable devices that assist enterprises in improving workplace safety levels	Classification
RQ2	Determining the critical parameters of LoRaWAN from the perspective of localization when planning a measurement campaign and processing its results	Open datasets; Dependencies
RQ3	Evaluating the potential for enhancing the accuracy of LoRaWAN-based localization through the optimization of localization algorithm	Dependencies; Algorithms

1.3 Thesis structure

Chapter 2 covers the first research question or **RQ1**. It discusses the IIoT paradigm, the role of wearables in it, their functions and metrics. The Chapter concludes with the choice of the research direction – localization performed by industrial wearable devices – and selects LoRaWAN for further analysis in this area.

RQ2 in this work is addressed through a comprehensive examination from both theoretical and practical perspectives, presented in Chapters 3 and 4, respectively. Chapter 3 discusses the reasoning behind selecting LoRaWAN for the localization-related investigation. and dives into the structure and architecture of this technology. The practical assessments are the subject of Chapter 4 that investigates the perspective of the LoRaWAN application as a solution for localization, utilizing datasets collected at Brno University of Technology, Czech Republic, and National University of Science and Technology Politehnica Bucharest, Romania. It describes the measurement campaigns, evaluates and processes the datasets, claims the precision of LoRaWAN-based localization for different types of environments under certain conditions.

Chapter 5 addresses **RQ3**, proceeding to look for the possibilities to increase the accuracy of LoRaWAN-based localization from the algorithmic point of view, proposing 2 k-NN based modifications.

Finally, Chapter 6 concludes the work by highlighting the results, summarising personal contributions, and considering the perspectives for future work.

Chapter 2

Technological State-of-the-Art

Starting from the general concepts, such as IoT, its niche IIoT, and wearable devices, this chapter leads the reader to the main topic of the current work – the application of the LoRaWAN technology for industrial applications using wearables. It adresses the first research question, presenting two classifications – on functions and collected metrics – as an outcome.

2.1 IoT, IIoT and wearable technology co-existence

The emergence of the IoT Paradigm dates back to the end of the 20th century. Generally, IoT is a system of interrelated things that have unique identifiers and communicate with each other. There are not many requirements to the "thing" (device) per se, as it could be any inanimate physical object, regardless of size or material, that has access to the Internet and connectivity solution making it widely spread in a tremendous variety of markets including healthcare, industries, sport, entertainment, work safety, beyond others [2], and promising to reach $27 billion connected devices by 2027 [3].

Among the variety of IoT devices, this study specifically focuses on wearables [4]. A wearable device is a smart electronic device in various shapes and sizes that is worn inside/on/near the body to collect and manipulate particular information. One of the most attractive features of wearables is multi-functionality: a single device can have several sensors and can usually perform a wide range of tasks. However, high functionality is commonly achieved at the expense of small size, low power consumption, mobility, and convenience for the user – at the price of other important features characterizing the wearable device. Thus, the main optimization problem in the field of wearable technology lies in the trade-off between its functionality and other practical features.

2.2 Industrial Wearables for work safety

The concept of **industrial wearable device** could be defined as a subcategory of wearables focused on the design, maintenance, monitoring, optimization, and analysis of manufacturing processes to gather real-time data and assist administrators/safety managers in making decisions. The main difference distinguishing industrial wearable devices into a separate class is the high requirements for solidity: industrial environments may be characterized by adverse conditions, such as very high or very low temperatures, extreme levels of humidity, etc. [5, 6]. In addition, in high-risk industries, there is an increased chance of physical damage to the device. Next, some work environments demand modernizing the precision, range, response time, and resilience of existing technologies. With the uniqueness of industrial wearable devices, people tend to be less careful when relying on technology. Thus, outages, imprecision, or delays in an industrial wearable device's work can cause an accident without emergencies or extreme conditions.

Classification on Functions

This work's first research question aims to identify the functionality of industrial wearables that allow enterprises to increase work safety levels. Considering the framework of the classification published [7], we offer an extended and modernized version already highlighted by the author in [5]. It consists of 4 main functions, monitoring, supporting, training, tracking, and 10 sub-functions and is summarized in Table 2.1.

To conclude, many risk factors in industries provoke an increase in work-related fatalities. However, wearable technology offers a wide range of functionality within industrial tasks and, expectedly, raises work safety standards.

Classification on Collected Metrics

It is worth noting that modern wearable devices are increasingly shifting towards multifunctionality, so most of them are equipped with not one but several sensors. Tables 2.2 and 2.3 outlined 23 common metrics in wearable technology: 15 body-related and 8 environment-related. However, not all of them are currently embedded in the industrial sector.

Table 2.1 Classification of Functions of Industrial Wearables [5]

Function	Sub-Functions & Description
Monitoring (M) Fitness trackers, smart rings, smart glasses, patches/ sensors attached to the body, smart clothing, implantable wearables, etc.	**Monitoring and control of vital parameters of workers**: measurement, systematization, and analysis of the physical (e.g., pulse, perspiration rate, etc.) or/and mental (e.g., fatigue, drowsiness) parameters of the employee in order to inform the employee himself and those responsible for safety in the industry about employee readiness for the work process [8, 9]. **Monitoring of environmental parameters at workplaces**: measurement, systematization, and analysis of the environment parameters (e.g., air quality, light intensity, etc.) to maintain conditions safe for work, promptly plan for evacuations, prevent disasters, ensure personnel with Personal Protective Equipment (PPE). Joint monitoring of human-related and environment-related parameters allows you to determine the degree of influence of the second factors on the first [10, 11].
Supporting (S) Exoskeletons, patches (to control the position of the body when lifting heavy objects), wearable robots	**Increasing the physical capabilities of the workers**: supporting the physical capabilities of the body to prevent injury during hard physical work [12–14]. **Facilitating communication and notification management**: ensuring a quick exchange of information on the territory of the working site without interrupting the work process (hand-free microphones, digital signage) [15, 16]. **Simplification of information management**: ensuring a secure transmitting, storage, displaying information, and fast access to documents and notifications [17]. **Facilitating the perception of industrial design**: creating virtual charts and graphs for easier perception using AR/VR helmets [18].
Training (Tn) Smart glasses, helmets, heads-up display	**Training of the workers**: tracking and notifying employees about the correctness of the actions (e.g., determining the correct posture using biomechanical analysis). Furthermore, training personnel in complex tasks in virtual and augmented reality before starting actual work reduces the risk of damage [13, 18].
Tracking (Tc) Smart bracelets, smart clothes, smart boots, digital pedometers, etc.	**Monitoring of location parameters of workers**: localization of workers allowing to effectively coordinate resources in the normal course of work and in cases of evacuations, as well as to limit illegal access to the workplace or equipment [19]. **Preventing struck by moving machinery:** tracking of object locations using proximity detection sensors to prevent collisions [10, 19]. **Creating a comprehensive picture of the whole production process**: providing a real-time map with employees, machinery, and equipment to facilitate decision making and distribution of workforce between sites [19].

Table 2.2 Human body-related metrics (NA – Accuracy is not specified for metric groups) [5]

Metric	Description	Example Accuracy	Examples
Blood oxygen saturation	The proportion of oxygenated hemoglobin relative to total hemoglobin in the blood (normal value: 90-100%).	70-100% [20]	pulse oximeters [21], skin patches [22]
Blood pressure	The pressure that blood puts on the walls of blood vessels. There are systolic or upper (normal value: less than 120 mmHg) and diastolic or lower (normal value: less than 80 mmHg) blood pressure [23]. The average working range of blood pressure sensors is 0–320 mmHg [24, 25].	86% [26]	Arm cuffs with attached sensors [27], cuff-less blood pressure sensors [28]
Calorie	A unit equals the heat needed to increase one gram of water temperature by one degree Celsius. There are several ways to calculate the number of calories (e.g., based on the number of steps or heart rate [29]), resulting in a wide range of wearables providing this function.	>91% (walking); >90% (running) [30]	Accelerometers, pressure sensors in fitness bracelets, smart shoes [29], etc.
Electrocardiogram (ECG)	The electrical activity of the heart [27], (Volts). It is one of the main tools for detecting heart problems (e.g., ischemic heart disease, arrhythmia) [31].	>90% [32]	Skin electrodes [27] in clothes [33], chest straps [34], etc.
Electroencephalogram (EEG)	The electrical activity of the brain [35] (Volts). EEG identifies and predicts brain-related diseases (e.g., Alzheimer's disease, epilepsy, dementia) [36]. In addition, it is also used for the emotion detection [37, 38].	>86% [37], [38]	Headset [35, 39]
Electromyography (EMG)	The electrical activity of the muscles [27] (Volts). EMG is used to track muscle fatigue and determine how quickly muscles recover from injuries [40, 41]	>90% [42]	Skin electrodes [27] embedded in bracelets, waist straps [43], clothes [44].
Eye blinks	Metric that envisages measurements of how fast and wide a person opens eyes. Eye blink measurements are used to identify the level of drowsiness using, e.g., Johns Drowsiness Scale [8] or Stanford Sleepiness Scale [45].	NA	glasses [8, 46, 45].
Glucose	The level of sugar in the blood, (grams per liter or moles per liter). High glucose level identifies diabetes, the symptoms of which are quite wide, ranging from visual impairment to increased fatigue and depressive episodes [47, 48]	>95% [49]	Strip-base [50], implantable [51] glucose sensors, smart tattoos [52]

Continued on next page

Table 2.2 – ***continued from previous page***

Metric	Description	Example Accuracy	Examples
Heart rate and pulse	Heart rate is the number of heartbeats per minute. Pulse is the number of vibrations of the aortic walls. Pulse may be a less accurate characteristic in pathologies (e.g., extrasystole) since not all heartbeats lead to the formation of a pulse wave [53]. Critical boundaries usually range between 40-200 beats per minute and depend on current activity, gender, age, health, type of activity, etc.	>76% [54]	Pulse oximeter [55], chest [56] and wrist straps [50], fitness bracelets
Heart sounds (murmurs)	Sounds that appear due to a change in blood flow, vibration of the surrounding heart tissues, and large vessels. Heart sounds can signal several different problems, including heart defects.	>80% [57]	Wrist band [57]
Location-related metrics	Metrics related to identifying the object's position: coverage, accuracy, power consumption, price of the wireless technology, etc.	NA	Wide range of wearables
Motion-related metrics	This metric refers to identifying the parameters of the human (in the context of this work) movements that are also called biomechanical analysis [58, 59]. Biomechanical analysis includes a wide range of functions such as determining the speed of movement, parameters of the respiratory apparatus, the correctness of performing physical activity, etc.	NA	Accelerometer, gyroscope [60], exoskeletons, pressure insoles, e-textile [58]
Perspiration or sweat	A liquid excreted from the skin's sweat glands [61]. Sweat is the second body fluid after the blood that contains the richest range of biomarkers like glucose, pH, cortisol, etc. [62].	>99% [63]	Sweat collectors, skin patches [62], smart watches [64]
Respiration rate (RR)	The number of inhalations and exhalations per minute. For an adult, the average RR is 16–20 breaths per minute [65]. The importance of RR monitoring that helps indicate respiratory diseases, including pneumonia, sleep apnea, etc., increased greatly over past years due to the pandemic COVID-19 [66].	>95% [66]	accelerometers, gyroscopes, piezoresistive RR sensors [66] skin patches [22]
Temperature	A measure of the ability of the body to generate heat [27]. However, the normal temperature range for a healthy human is 36.16–37.02 °C [67], and the widest recorded range is 24–44 °C [68], usually the range of the wearables measuring temperature is wider.	>99% [69]	Temperature sensors [70, 71] and skin patches [72]

Table 2.3 Environment-related metrics [5]

Metric	Description	Examples
Air Quality Index (AQI)	An index shows the degree of air pollution in a certain area [73]. This indicator is determined by the registered concentrations of pollutants in the air and varies from 0 to 500. Based on the indicator value, the environment is assigned one of 5 (or 6) hazard classes: from good to dangerous. Depending on a person's physical characteristics, pollution levels above 101 can already cause significant damage to health, increasing the risk of developing pneumonia, lung cancer, etc. [73]	Gas sensors (e.g., CO2 sensor [74])
Atmospheric pressure	The pressure exerted by the weight of the atmosphere on the surface below it [75] (hectopascals, hPa). For professions in conditions of low or high barometric pressure (for example, pilots and divers, respectively), this parameter is essential since, from a long-term perspective, they may be associated with the development of respiratory, heart, neurological changes, decompression illness, etc. [76, 77] On average, the measurement range of pressure sensors is from 300 to 1100 hPa with an error of 0.5 hPa.	BMPxxx sensor group [74], barometers embedded in bands, smartwatches, glasses [78], etc.
Light intensity	Light strength produced by a specific lamp source measured in lux [79]. The National Optical Astronomic Observatory [80] has released recommendations for light intensity in various situations. Improper illumination can negatively affect worker safety both directly (impaired vision, cancer, sleep disturbances, etc. [81, 82]) and indirectly (increased chance of accidents in poorly lit work sites such as mines and tunnels [83]).	Motion, traffic, ambient light sensors [84], e.g. [85]
Noise level	The amplitude level of the undesired background sound [86] (dBA). Constant sound above 80 dBA leads to physiological effects, and above 100 dbA—to the hearing damage, [87].	Sound sensors, dynamic microphones [84].
Radiation	An energy from a nuclear reaction [88] (Sievert (Sv) or roentgen equivalent man (rem)). Even a relatively safe dose of radiation (<5 rem or 0.05 Sv [89]) with time can cause permanent health problems like cancer. High doses lead to the vomit, skin burns, death [90]	Radiation detectors [91]
Relative Humidity	The amount of water present in the air compared to the greatest amount it would be possible for the air to hold at that temperature [92]. The hygienic norm of relative humidity for humans is 30–60%. Low humidity causes the body to become dehydrated and increases the possibility of bacteria invading the human body. High humidity can lead to overheating, increased sweating, and the emergence of allergens (mold, fungi, dust mites) [93, 94].	Temperature/ humidity sensors [95]

Continued on next page

Table 2.3 – ***continued from previous page***

Metric	Description	Examples
Temperature	Ambient temperature, which is most often expressed in degrees Celsius. The typical range of temperature sensors is -40 to 125 degrees Celsius °C [62]. The survival limit for the person is between -40 °C [96] and 48 °C. For the best performance, the optimal ambient temperature is 22–26 °C [97].,	Temperature/humidity sensors [62, 95]
Ultraviolet index (UVI)	A dose of ultraviolet radiation from the sun at a particular time and place. Currently, UVI can be identified based on the linear scale divided into 5 ranges: low (UV: 1–2), moderate (3–5), high (6–7), very high (8–10), extreme (11+) [98]. The sun exposure to UV higher than 7 can lead to serious damage to the eyes (e.g., snowblindness), skin (burns, skin cancer, skin aging), and overall immune system [99].	UV radiometers and dosimeters embedded in wrist bands, smartwatches, clips, etc. [100]

The industrial conditions define the choice of wearable devices and, consequently, the metrics that can be collected. Thus, when talking about environment-related data, the most requested metrics in the literature are temperature, relative humidity, and air quality.

2.3 Chapter conclusions

This chapter presents to a reader a brief introduction into industrial wearable device, revealing the main concepts and proposing two classifications – on functions (Table 2.1) and metrics (Tables 2.2– 2.3) of industrial wearables, addressing the first research question set for this work.

Considering the current challenges in the field that we have published in [5], we selected the top area of interest at the junction of localization and connectivity clusters as one of the most sharply outlined issues. Following this path, further work was shifted to investigating the LPWAN technologies, particularly one of its most significant representatives, LoRaWAN, which is widely used as a connectivity solution, however, is considered unsatisfactory for localization purposes. The direction of the research, thus, is being narrowed to exploring the potential of LoRaWAN as a unified solution for the IIoT sector.

Chapter 3

LoRaWAN Technology Analysis

This Chapter reminds the main concepts behind LoRaWAN technology, discusses the main directions of its utilization in modern applications, and compares it with other LPWAN technologies, justifying its choice for study and use in the IIoT area in this work. Further, it investigates practical cases and theoretical perspectives of applying LoRaWAN technology as a communication solution and a solution for localization, touching on the first part of RQ2.

Low-Power Wide-Area Network (LPWAN) technologies are a popular choice for IoT applications that require long-range communication with low power consumption. As the IoT industry grows, so does the number of LPWAN technologies available: according to estimations in [101], during the next 7 years, the LPWAN market promises to grow with a significant CAGR of 64.7%. The key points leveraging the expansion of this technology cluster are strived to cover distant areas and rising interest in smart metering and smart cities concept, which exploits Each LPWAN technology has its unique features, advantages, and disadvantages, making it essential to understand their differences to choose the best solution for a particular IoT application.

Currently, LPWAN is represented on the market mainly by four leading technologies: LoRaWAN, Sigfox, LTE, and NB-IoT. The choice between LPWAN technologies is challenging and application-dependent. From the localization point of view all four leading LPWAN technologies is on the same level - starting from 100 meters. Therefore, in the process of choosing a technology for further research, it was decided to primarily focus on the frequency of applicability of the technology for industrial purposes. Thus, the focus was narrowed down to Sigfox and LoRaWAN, and the choice was made in favor of the latter due to its higher availability and general convenience (bigger bandwidth, better scalability, open protocol, easier network customization, bigger community).

3.1 LoRaWAN Architecture

LoRa

LoRa stands for Long Range and refers to the physical layer of LoRaWAN or modulation technology that Semtech patents. It is based on the spread spectrum modulation cluster method known as Chirp Spread Spectrum (CSS).

Generally, we can talk about four parameters specific to LoRa initialization:

- **Central frequency**.
- **Bandwidth (BW)**.
- **Spreading Factor (SF)**. According to the Semtech documentation, SF is the logarithm in base 2 of the number of chips per symbol. LoRa allows to configure six SFs: 7, 8, 9, 10, 11, and 12.
- **Code Rate (CR)**. There are 4 CRs commonly utilized in LoRa: CR1 or 4/5 (4 information and 1 error correction bits), CR2 or 4/6, CR3 or 4/7, and CR4 or 4/8.

To summarize, when talking about LoRa, one refers either to the modulation method or to the physical layer of LoRaWAN technology. The second essential part of the technology's stack, the LoRaWAN protocol, will be presented in the following subsection.

LoRaWAN

LoRaWAN is an open protocol built on top of LoRa PHY. The LoRaWAN specification does not define any particular modulation technology. However, it is safe to say that LoRa is the most widely used [102]. The infrastructure of a LoRaWAN network comprises several main components: end devices (ED), gateways (GW), and network servers (NS). Additional elements may include a specialized network join server (NJ) to facilitate network roaming. GW and NS are commonly connected through an IP-based interface. The functionality of NS and the user application programming interfaces (APIs) may vary depending on the network operator. The network architecture of LoRaWAN adopts a star topology, wherein the end devices exclusively communicate with LoRaWAN gateways and do not have direct peer-to-peer communication with one another.

In short, the LoRaWAN network could be described as follows: the transmission is initiated by the EDs using an Aloha-like channel access mechanism. In other words, the ED initiates communication at any time while adhering to the operational restrictions of the selected radio channel. EDs send collected data to the GWs, which, in turn, sends the data to an NS. A basic LoRaWAN network typically consists of a single GW and the NS that can be integrated into the GW. The network server analyzes the received data and eliminates redundant packages. Only the chosen data packets are then forwarded to the application server.

3.2 Theoretical LoRaWAN coverage assessment

The coverage estimation is an essential part of the work, which provides an idea of what signal strength can be expected at a certain distance. As mentioned earlier, LoRaWAN is one of the longest-range communication technologies, claiming to have up to 50 km in rural areas. This subsection is targeted at a provision of theoretical assessment of the LoRaWAN coverage, using 4 widespread path-loss models: Okumura-Hata, Okumura-Hata COST 231 [103], 3GPP UMa [104], and 3GPP 3D-UMA [105].

For the theoretical range assessment, we chose the default parameters of LoRaWAN devices (*8 GWs, 7 MPs, SF7/12, 14 dBm of nominal Tx/Rx power, 2.15 dBi of antenna Tx/Rx gain, dipole antenna*), identified the common applicability limits for all 4 models, and calculated the RSSI dependency on the distance (see Figure 3.1).

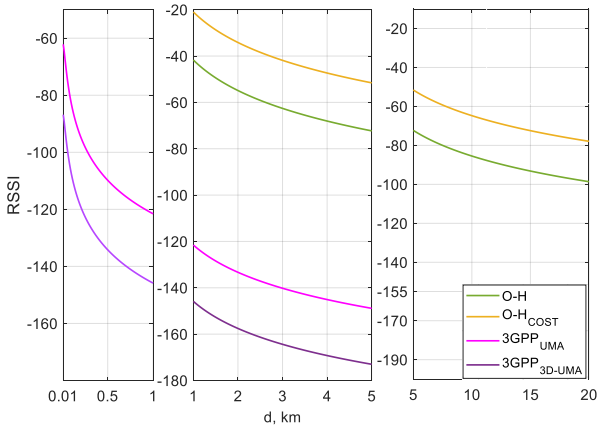

Fig. 3.1 Theoretical range assessment of LoRaWAN ($h_{TX} = 1.5m$, $h_{RX} = 30m$, $SF = 12$)

The chart shows that despite the identical dynamics of the studied path-loss models on the joint section (a 30 dBm drop between 1 to 5 km), the Okumura-Hata models assess the potential of LoRaWAN as being 80–100 dBm more optimistic than the UMa models. Thus, according to the Okumura-Hata case, we can expect reception transmission up to distances of 20 km with the smallest SF7 (maximum RX sensitivity -123 dBm) leaving some margin. On the other hand, calculations carried out based on UMa and 3D-UMa models claim that communication will only be possible for 0.5–1 kilometer at the highest SF (maximum RX sensitivity -137 dBm). Thus, which of the models is closer to reality remains an open question and will be addressed within this framework during the practical assessment of the coverage of the technology.

3.3 Simulation-based LoRaWAN coverage assessment

To provide a comprehensive view of the coverage assessment for LoRaWAN technology, this subsection explores the capabilities of well-known simulators and presents simula-

tion results using the HTZ Communications software environment, a complex tool that estimates coverage of the most common-use communication technologies, using more than 50 propagation technologies for indoor and outdoor scenarios.

An outdoor area near Building A and B at UNSTPB, featuring 5 LoRaWAN transmitters, was selected for simulations. The RSSI will be registered at 8 distributed inside the university on the different floor points where the LoRaWAN receivers (GWs) will be placed. The setup is shown in Figure 3.2), while for the simulation parameters we used *8 GWs, 7 MPs, SF7/12, 14 dBm of nominal Tx/Rx power, 2.15 dBi of antenna Tx/Rx gain, dipole antenna, Okumura-Hata COST 231 propagation model*. No additional parameters, such as weather or time of day, were considered during the simulation.

Figure 3.3 shows an RSSI analysis at the control points—locations where the gateways will be installed for practical experiments—showing an average RSSI of ∼-90 dBm for SF7 versus ∼-50 dBm for SF12.

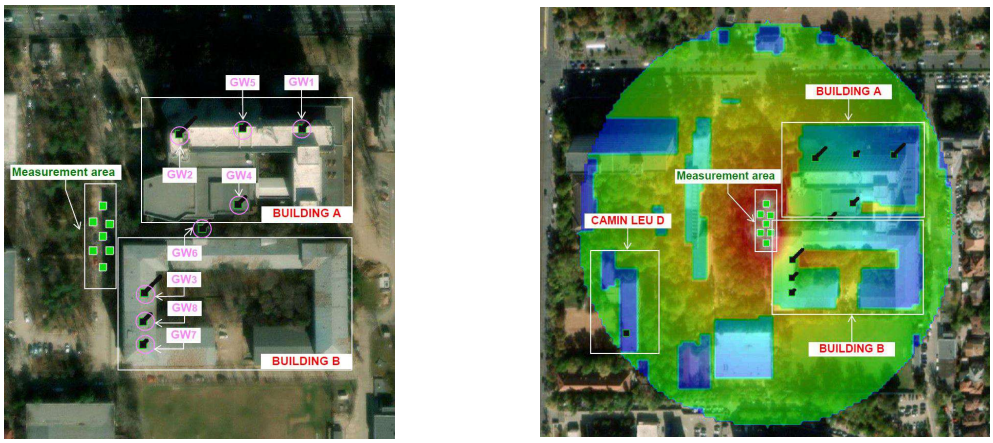

a) b)

Fig. 3.2 LoRaWAN simulation: a) setup, b) simulation (radius = 150 m)

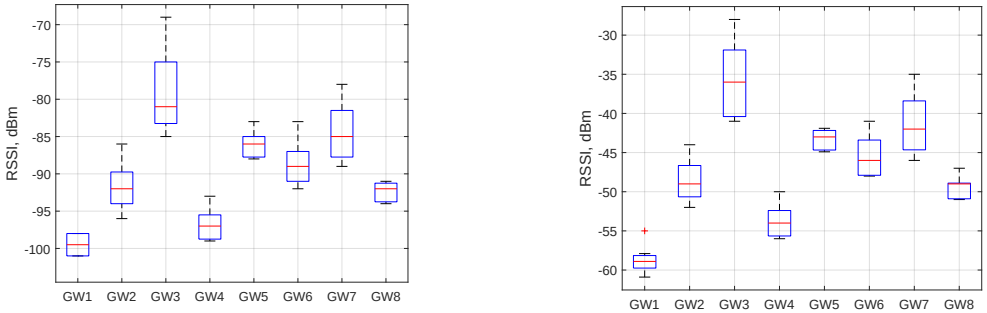

a) b)

Fig. 3.3 HTZ, Distribution of RSSI: a) SF7 (125 kHz), b) SF12 (125 kHz)

Without the ability to compare the simulation results at the gateway points with the theoretical signal propagation assessment using the Okumura-Hata models directly, we will utilize the 3GPP UMa models for comparison. Since the presented simulation is

limited by 150 m, according to the UMa/3D-UMa theoretical analysis (Figure 3.1), one should expect a signal at the boarder of around -90/-110 dBm at SF12, respectively. At the same time, practically, the green zone at the boarders of the simulated area in Figure 3.1 corresponds to the RSSI $\sim$-50dBm, i.e., 40/60 dBm higher than for the models UMa/3D-UMa, respectively.

3.4 Chapter conclusions

This Chapter opens the discussion of the second research question: determining the critical parameters of LoRaWAN from the perspective of localization when planning a measurement campaign and processing its results. First, it elaborates on the choice of LoRaWAN technology for the stated problem; then it is trying to assess LoRaWAN network coverage from the theoretical and simulation standpoints:

- For the **theoretical network coverage assessment**, the work offers a nuanced estimation of signal strength across varying distances utilizing known path-loss models like Okumura-Hata, Okumuara-Hata COST 231, 3GPP UMa, and 3GPP 3D-UMa. The analysis indicates that while all studied path-loss models show similar trends, the Okumura-Hata models provide a more optimistic assessment of LoRaWAN's potential, predicting possible communication up to 20 km under specific conditions, compared to the UMa models' 0.5–1 km range.

- For the **simulation-based network coverage assessment**, the work utilizes HTZ Communication environment - a complex tool allowing designing the network across a broad frequency spectrum ranging from 1 kHz to 1 THz. The simulation setup was planned and executed in a $\sim$ 50,000 square meters area, Bucharest, Romania, with the intention of its subsequent replication during the practical experiment. The Okumura-Hata COST 231 model, which yielded the most optimistic results in theoretical analysis, was selected, keeping in mind that 3GPP UMa models are currently unavailable in HTZ.

  The LoRaWAN coverage simulation for a targeted area with SF7 and SF12 within a 150 m radius revealed through a color map that SF7 has limited building penetration, with some areas showing no coverage. The color scale difference indicates that RSSI for SF12 is significantly higher (30-40 dBm) than for SF7, suggesting that a higher SF is more suitable for indoor applications.

Due to the inability to compare the simulation results with the theoretical ones for Okumura-Hata models (unavailable at distances below 1km), we compared them with theoretical 3GPP UMa models. The comparison revealed a substantial discrepancy in signal levels: theoretical analysis suggested -90/-110 dBm, while simulation results indicated -50 dBm. Overall, the accuracy of the inspected models, particularly for short distances and urban settings, remains to be validated through practical assessments.

Chapter 4

Experimental analysis of LoRaWAN-based localization

This Chapter covers the practical part of RQ2 and reveals the details of organizing and carrying out the measurement campaigns, analyses the results, calculates and claims the accuracy for LoRaWAN-based localization for the particular cases in the three types of environment: indoor aboveground (iAG), indoor underground (iUG), and outdoor.

4.1 Measurement campaign description

Two comparable measurement campaigns (MC) in BUT, Czech Republic, and in UNSTPB, Romania (Figure 4.1) were set up to identify the localization accuracy that can be achieved using LoRaWAN technology. Together, campaigns cover the most common industrial scenarios, providing datasets for indoor Above-Ground (iAG), indoor Underground (iUG), and outdoor environments.

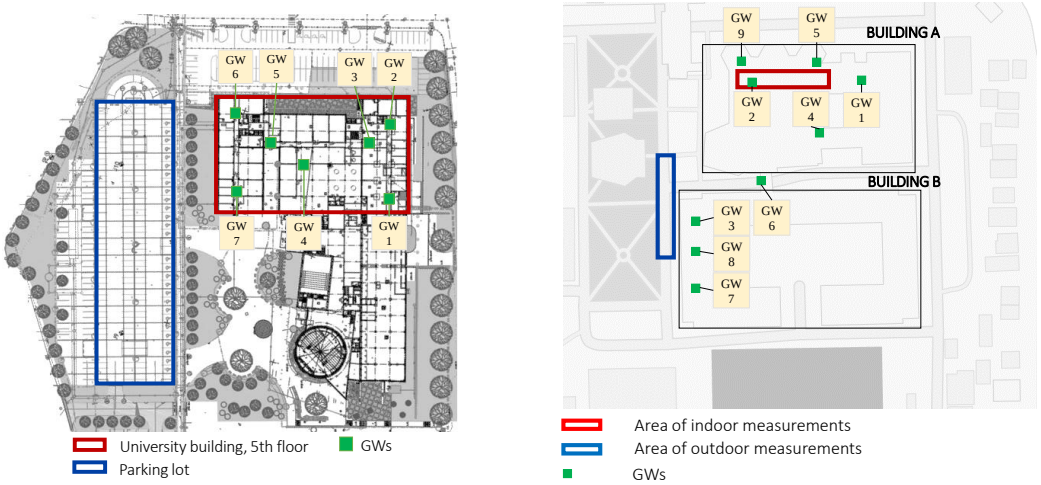

a) b)

Fig. 4.1 Measurement environment: a) BUT, b) UNSTPB

The first MC was organized at BUT, Czech Republic. It considers two cases: iAG collected on the 5th floor of Faculty of Electrical Engineering and Communication (FEEC) building (red rectangular in Figure 4.1 (a)), and iUG collected on the underground parking lot (blue rectangular in Figure 4.1 (a)) [1].

Romania's University Politechnica of Bucharest (UNSTPB) was selected as the second location. This MC reviews another indoor aboveground case, using Faculty of Electronics, Telecommunications and Information Technology (ETTI) buildings (Building A and B in Figure 4.1 (b)) and an outdoor case arranged on the alley in front of the buildings (blue rectangular in Figure 4.1 (b)).

Both MCs were planned similarly, i.e., involving the same type of equipment and the same procedure. As an equipment we used LoRaWAN GW LG308 (9 pieces), Field Test Device (FTD) [106] (2 pieces) aad an auxiliary equipment such as routers (for Internet connection of LoRaWAN GWs) and wire extensions. In this work, we have collected five open-access fingerprinting datasets using LoRaWAN technology for two measurement campaigns. All cases and related parameters are listed in Table 4.1.

Table 4.1 Investigated scenarios

Place	Measurements	Equipment	MPs	Spacing, m	SFs	GWs	Environment
BUT	Building	Building	203	1	7, 9, 10, 12	7	iAG
BUT	Parking (2 floors)	Building	147	2.5	7,12	7	iUG
BUT	Parking (2 floors)	Parking	147	2.5	7,12	6	iUG
UNSTPB	Building	Building	155	1	7,12	9	iAG
UNSTPB	Alley	Building	155	1	7,12	8	outdoor

The following part of the chapter is dedicated to the scenarios presented in Table 4.1: it describes the coordinate systems, area, and equipment placement, analyzes the nature of collected datasets, calculates the mean localization errors, and discusses the perspective of LoRaWAN technology as a localization solution.

4.2 Indoor aboveground campaign

BUT indoor aboveground dataset

Location: measurement setup was located on the 5th floor of seven-storey FEEC building of BUT (Figure 4.1). The internal concrete walls are 150 mm wide. Figure 4.2 shows the **measurement map** developed for this scenario. The MPs were distributed over 4 corridors: similar left and right corridors (50 × 1.8 m), central corridor (36 × 1.8 m), and

[1] Map is available online: https://en.mapy.cz/s/davubejanu

horizontal corridor (75 × 1.8/3.2 m). Along the walls of each corridor are iron benches, and the horizontal corridor has two separate sections with stairs and lifts.

MC parameters: there are 203 MPs, separated by a distance of 1 meter. 3 UL signals were sent from each MP using FTD configured for a certain SF (7, 9, 10, or 12) to 7 available GWs with identification numbers 1-7. The GWs were placed on the floor. Overall, signal maps for 4 SFs took 4 days: datasets for SF7 and SF12 were gathered during the evenings, and for SF9 and SF10 – during the mornings.

Statistical analysis. The Figure 4.3 shows RSSI distributions and the average RSSI level for SF7 and SF12. At average RSSI values fluctuate around -86 dBm (SF7: -83.5 dBm; SF9: -86.4 dBm; SF10: -85.7 dBm; SF12: -88.1 dBm).

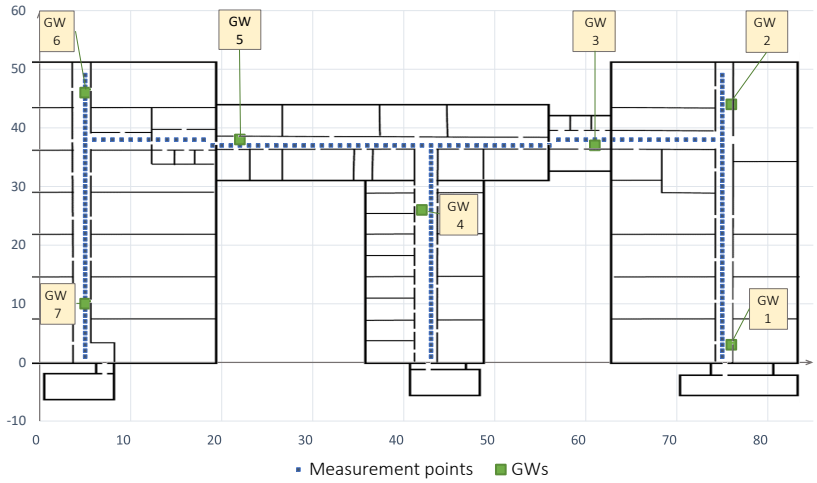

Fig. 4.2 MC in BUT, office: coordinate system

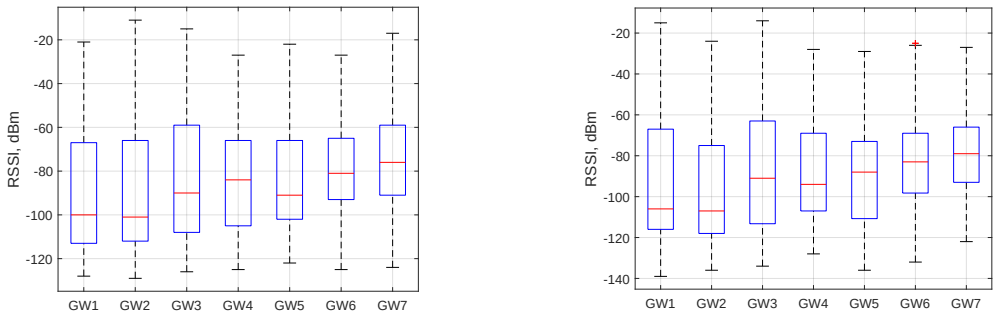

a) b)

Fig. 4.3 Distribution of RSSI: a) SF7, b)SF12

UNSTPB indoor aboveground dataset

A comparable MC was conducted in Bucharest, Romania, to have more reliable data for analysis and solid conclusions.

Location: open space rectangular measurement area (5 × 31 m) was arranged on the ground floor of Building A of the Faculty of Electronics, Telecommunications

and Information Technology (Figure 4.1). The GWs were distributed over eight-story buildings A and four-story buildings B with concrete walls. The **measurement map** is shown in Figure 4.4.

MC parameters. In this case, the area was divided between 155 MPs. Similarly to the previous case, spacing equals 1 meter, and 3 signals were sent from each MP. Since the analysis of the previous case did not show any significant dependence of localization accuracy on the SF, it was decided to reduce the investigation of the SF just to its extreme possible values – 7 and 12. In contrast, to better study the dependency of accuracy on GWs, their number was increased from 7 to 9. The distribution of the GWs among the considered area is presented in Figure 4.1 and Table 4.2. This measurement campaign took 3 days.

Table 4.2 Distribution of the GWs (MC in UNSTPB)

GW	Location
1	Building A, 3rd floor
2	Building A, 3rd floor
3	Indoor: Building A, ground floor; Outdoor: –
4	Building A, ground floor
5	Building A, 1st floor
6	Passage between Building A and B, 1st floor
7	Building B, ground floor
8	Building B, 3rd floor
9	Building B, 1st floor

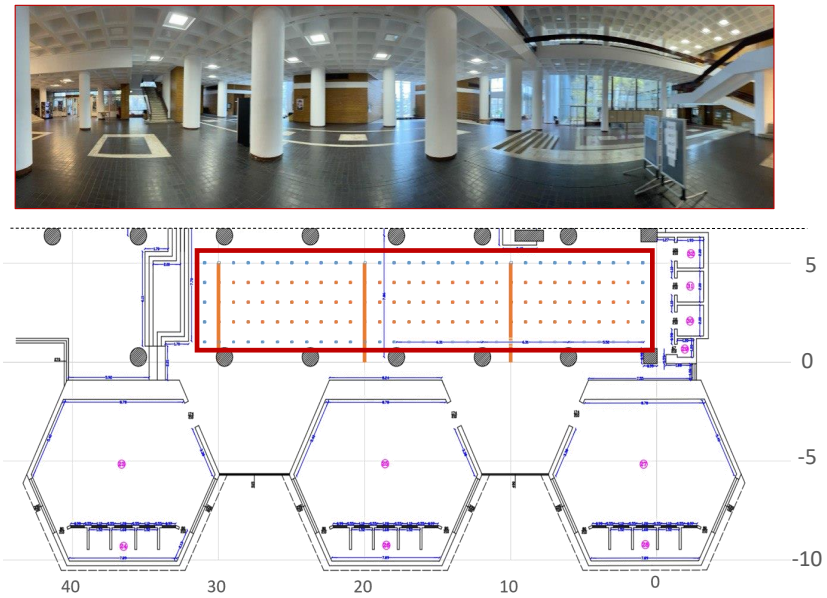

Fig. 4.4 Measurement campaign in UNSTPB: indoor environment

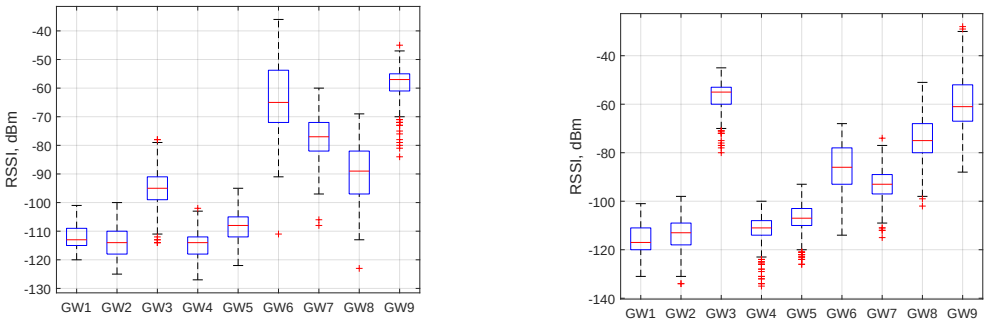

a) b)

Fig. 4.5 Distribution of RSSI (MC in UNSTPB, indoor): a) SF7, b) SF12

Statistical analysis. The average acceptance probability for this dataset equals 92.6%. This result is comparable to the previous indoor scenario (94%): even though we were dealing with open space in this case, unlike the corridors in the previous scenario, the GWs were located much further away).

Figure 4.5 shows RSSI distributions and the average RSSI level for each SF. On average, RSSI values fluctuate around -90 dBm (SF7: -89.8 dBm; SF12: -90.6 dBm), which is also comparable with the previous scenario (-86 dBm, see Figure 4.8). Despite the cases having different initial parameters (see Table 4.1), this gives us more rights to compare them.

4.3 Indoor underground campaign

The usability of the LoRaWAN as a communication technology for underground sites was explored in several works such as [107–109]. Work published in [110] investigates the performance of LoRaWAN technology and NB-IoT in challenging environments, including the underground ones. However, to the best of the author's knowledge, a study needs to investigate the possibilities of LoRaWAN technologies for localization in the underground environment. During the research, it was decided to pay attention to this fact and use two levels of underground parking near BUT, Czech Republic, as an approximate analog of the underground environment being used in the mining industry.

In the work, we used the same measurement area two times for different setups: in the first case, GWs were distributed in the same as in the BUT indoor case – on the 5th floor of the office building (see Figure 4.2), in the second case GWs were placed locally – on the bottom floor of the parking lot. Comparison of these two cases allows us to analyze how the probability of acceptance of the signal and localization accuracy depends on the remoteness of the GWs from the measurement area.

Location. 30 cm wide parking lot's walls are made of concrete. There are two levels in the parking lot that we are interested in, located one below the other and 2.8 meters

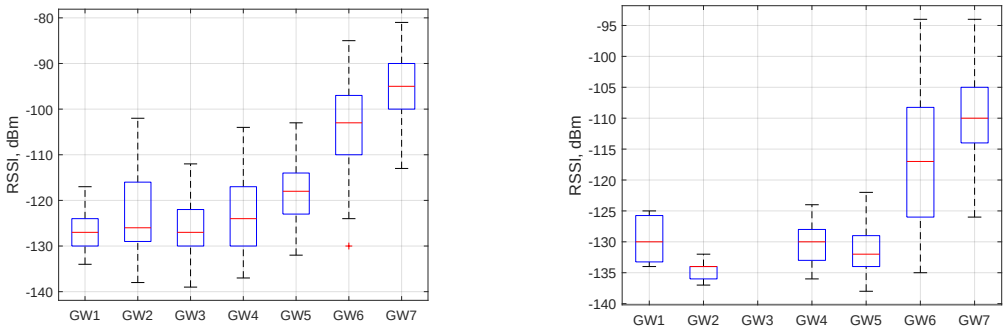

a) b)

Fig. 4.6 Distribution of RSSI (MC in BUT, indoor, GWs in the building): a) top floor (2), b) bottom floor (3)

high each. During the measurements, the top and bottom floors were filled to 74 and 10 percent, respectively.

Indoor underground dataset: GWs deployed in the building

The **MC parameters**. As was mentioned, the setup is the same as in the BUT iAG scenario. The FTD was configured to two SFs: 7 and 12. The **measurement map** for this scenario was partially described in our work [111]: it consists of 49 MPs placed in a line with a spacing of 1 m (see Figure 4.7).

Statistical analysis. The difference in 1 floor resulted in a 30% difference in the probability of signal acceptance (58.9% and 28.8% at the average for the top and bottom underground floors, respectively). Moreover, in this experiment, due to the specific underground hard-to-penetrate environment, we can more clearly observe the difference between SF 7 and 12: in the latter case, the probability of acceptance at average higher by 10-15%. The distribution of RSSI for this case is shown in Figures 4.6 (for SF12).

Indoor underground dataset: GWs deployed locally

MC parameters. The next experiment used the same measurement area, but GW was deployed directly on the parking lot on the bottom floor. The same **measurement map** was used as in the previous case: it has 49 MPs located 1 m from each other. The underground setup was considerably harder to organize owing to the infrastructure specifics. Therefore, this case involved just 6 GW out of 7 available (see Figure 4.7).

Statistical analysis. Probability to receive a signal, in this case, is more comparable to the indoor scenarios and equals 95.2% and 90.1% for the top and bottom floors, respectively..

Figure 4.8 shows the RSSI distributions for both, top (SF7: -78.8 dBm; SF12: -79.2 dBm) and bottom (SF7: -67.7 dBm; SF12: -66.9 dBm) floors. As anticipated, the difference between the average RSSI levels obtained using SF7 and SF12 becomes less

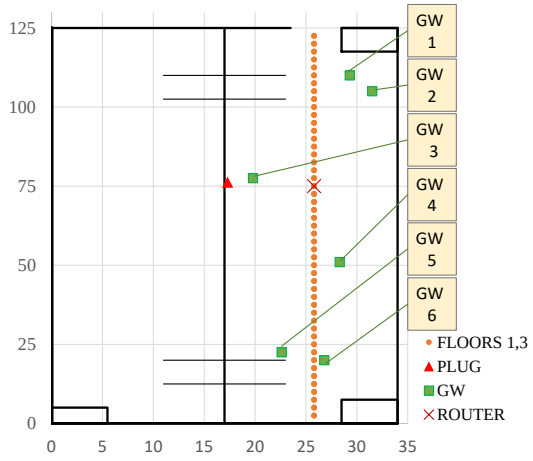

Fig. 4.7 Coordinate system for MC in BUT, parking lot

obvious at closer distances: less than 1 dBm in this example against 3–4 dBm – in the previous one described in subsection 4.3 (see Figure 4.6).

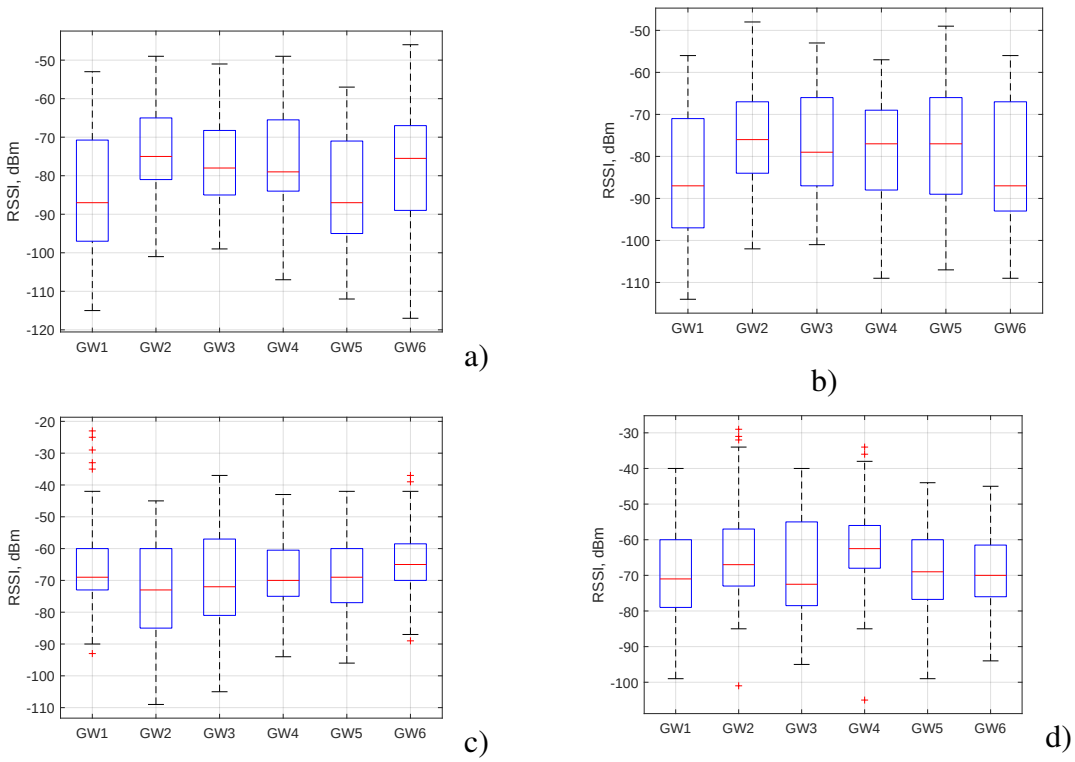

Fig. 4.8 Distribution of RSSI (MC in BUT, indoor): a) SF7, top floor (2), b) SF12, top floor (2), c) SF7, bottom floor (3), d) SF12, bottom floor (3)

4.4 Outdoor campaign

Location. In our work, we are considering just one scenario involving an outdoor environment – the open space area in front of the ETTI department of UNSTPB. The

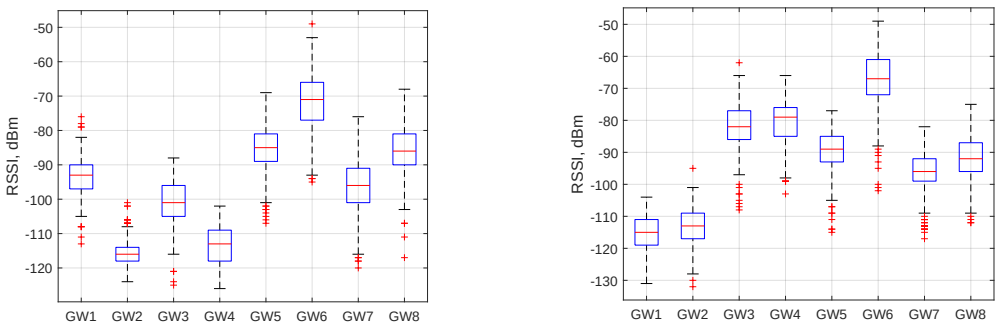

a) b)

Fig. 4.9 Distribution of RSSI (MC in UNSTPB, outdoor): a) SF7, b) SF12

measurement map is the same as for indoor aboveground measurements in BUT (see subsection 4.2): 5 rows of 31 MPs each with a spacing of 1 m between them (Figure 4.4). The only exception is the location of GW5, which has been moved to a more remote building behind a small park and another building. The measurement process itself took 2 days.

Statistical analysis. The average acceptance probability for this dataset equals 91%, which is slightly less (by 1.6%) than for almost the same setup in iAG UNSTPB scenario. Such a result confirms the expectations: equipment setup is almost the same, and areas are located approximately 50 m from each other.

Returning to the comparison with the indoor case, it should be noted that the RSSI distribution's shape appears to be more normalized than in the indoor case despite the mean RSSI level being almost the same (SF7: -92.6 dBm; SF12: -90.5 dBm) (see Figure 4.9).

4.5 Selected numerical results

For the collected datasets described in subsections 4.2-4.4, we calculated the localization error using Root Mean Square Error (RMSE).

The most valuable results were combined in Figure 4.10, which shows LoRaWAN localization accuracy estimation for all the investigated scenarios. As can be seen, trilateration and WCA provide a very low accuracy within a few tens of meters, which makes these methods useless for localization purposes. Trilateration and WCA levels are presented just for the first dataset to avoid overburdening the graph. At the same time, *k*-NN/*k*-NN-W give much better and generally relatively optimistic results for most of the scenarios, especially for both indoor aboveground scenarios (ds1 and ds6), registering an accuracy of 2-3 meters – 10 times less than was provided by trilateration. Figure 4.11 integrates the most successful, in terms of a minimum localization error, combinations of the parameters (algorithm (*k*-NN/*k*-NN-W), redundancy reduction strategy (maximum/averaging)) for all the cases.

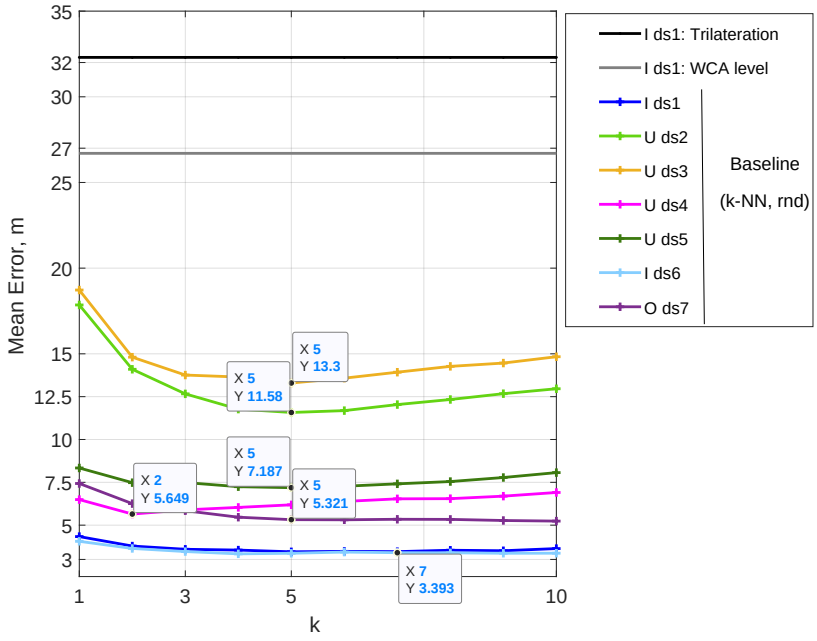

Fig. 4.10 Localization accuracy for baseline (conventional *k*-NN without preprocessing)

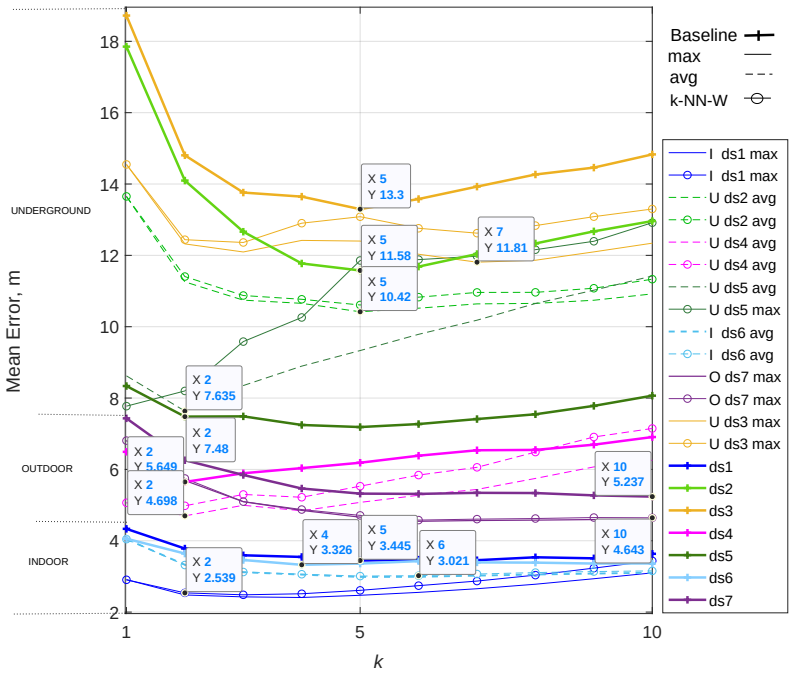

Fig. 4.11 Localization accuracy for comparison *k*-NN-W and *k*-NN

The summary of the results presented in Table 4.3 shows the average accuracy of 2.7 m for the indoor environment and 4.56 – for the outdoor.

Table 4.3 Minimal mean localization errors for investigated scenarios (averaging redundancy reduction strategy)

Place	Measurements	Equipment	Spacing, m	GWs	Env.	ds№	Min mean error,m	Method
BUT	Building	Building	1	7	iAG	ds1	**2.54**	*k*-NN/*k*-NN-W
BUT	Parking	Building	~ 3	7	iUG	ds2; ds3	**10.42 (fl. 2); 11.81 (fl. 3)**	*k*-NN
BUT	Parking	Parking	2.5	6	iUG	ds4; ds5	**4.70 (fl. 2); 7.63 (fl. 3)**	*k*-NN
UNSTPB	Building	Building	1	9	iAG	ds6	**3.02**	*k*-NN/*k*-NN-W
UNSTPB	Alley	Building	1	8	outdoor	ds7	**4.64**	*k*-NN/*k*-NN-W

4.6 Chapter conclusions

Summarizing this chapter ans combining it with the conclusions previously made in [112], we can draw the following key points:

- **Localization approach**. Trilateration and WCA turned out to be unsuitable, providing an error of 27-32 m, while *k*-NN and *k*-NN-W can reduce this number up to 10 times depending on the dataset. Comparing *k*-NN with *k*-NN-W, one can notice that, on average, a basic option slightly outperformed an extended one.
- **Redundancy reduction**. The baseline *k*-NN, i.e., *k*-NN with the random selection of a fingerprint, is noticeably outperformed by averaging and selecting the fingerprint with the maximum RSSI. In turn, the maximizing strategy was marginally surpassed by averaging one.
- **Environment**. Of all the options studied, the highest accuracy is observed for the indoor dataset, followed by the outdoor and underground datasets.
- **Propagation model**. The comparison of the practice with the theory and simulation carried out in Chapter 3 did not provide a clear answer as to which of the four studied models suits the best. From the perspective of the dynamics of signal level change from GW to GW, the Okumura-Hata model appears to be quite precise while overestimating the overall RSSI level. On the other hand, the UMa model matches general RSSI-level expectations.

To make a more consistent conclusion regarding the possibility of using LoRaWAN for localization purposes using RSSI, a more detailed study related to the processing step, i.e., localization approaches, should be carried out. This problem and, concurrently, the third research question of this work is addressed in the next chapter.

Chapter 5

Improving LoRaWAN Localization Accuracy

The discussion of the prospects of LoRaWAN RSSI-based localization for use in the industrial wearable sector continues in this chapter: It focuses on the 3rd research question, exploring the processing phase (i.e., comparing several localization approaches) and presenting 2 modifications of the k -NN approach aimed at improving precision.

5.1 Improved-accuracy algorithm proposal

Modification 1: Reassessment from the origin

The first modification strategy proposes to reassess the relevance of the chosen nearest neighbors based on the Euclidean distance between them and the origin points. As an origin point, one of the corners of the perimeter of the measurement area can be chosen. The idea behind this strategy is that the group of the nearest neighbors should be more or less in the same zone. Thus, the proposal is to estimate Euclidean distances from the origin to each neighbor, identify an approximate localization zone based on mean distance value, and neglect outliners, i.e., those neighboring points outside this zone.

The obvious disadvantage of this strategy is that the distance from the origin does not define a specific value but draws a circle, each point of which represents a possible value. We introduced the second origin point to reduce the localization area and, consequently, decrease the probability of choosing a not-relevant neighbor.

Another point that supposed to be discussed is the minimal k, for which this strategy might be useful: obviously, for the small group of neighbors the proposal will not work, since it takes statistical mean as an assessment baseline. In this work, k_{min} will be determined empirically: following the same scenario as in Chapter 4, we will calculate the mean localization error for $k = [1, 10]$ and compare the results with the original k-NN.

Summarizing information above, let us formalize the algorithm:

1. Calculation of k-NN (-W).

2. Calculation of the Euclidean distances between each k neighbors and origin points:

$$dist_{o1,2k} = \sqrt{(x_{o1,2} - x_k)^2 + (y_{o1,2} - y_k)^2}, \tag{5.1}$$

   where (x_o, y_o) are the coordinates of the origin point and (x_k, y_k) - coordinates of the kth nearest neighbor.

3. Calculation of the mean values $\bar{dist}_{o1k}$ and $\bar{dist}_{o2k}$:

$$\bar{dist}_{o1,2k} = \frac{\sum^k dist_{o1,2k}}{k}, \tag{5.2}$$

4. Setting borders to limit localization zone: $\bar{dist}_{ok} \pm \Delta$, where Δ is a tolerance. In this work Δ = 30 (modification 1) and 50% (modification 1.1), where σ is a standard deviation.

5. Identification of neighbors which are not in the localization zone. If no outliners were found, the algorithm exits. The result of the algorithm is the last evaluation of the position.

6. Elimination of outliners.

7. Position update: calculation of the average coordinates of the remaining neighbors.

Modification 2: Reassessment from the estimated value

The second modification is similar to the first one. However, the calculation of Euclidean distance is performed from each neighbor not to the origin point but to the preliminary estimated value given by k-NN. The localization zone, in this case, will be determined by one border and stretched between 0 and the mean value of the Euclidean distances plus allowance.

Thus, the overall algorithm is as follows :

1. Calculation of k-NN(-W).

2. Calculation of the Euclidean distances between each k neighbor and origin point:

$$dist_{ek} = \sqrt{(\hat{x} - x_k)^2 + (\hat{y} - y_k)^2}, \tag{5.3}$$

   where ($\hat{x}$, $\hat{y}$) are the coordinates of the value estimated via k-NN approach and (x_k, y_k) – coordinates of the k_{th} nearest neighbor.

3. Calculation of the mean value $\bar{dist}_{ek}$.

Table 5.1 Relative advantages of proposed strategies without preprocessing over the baseline

Strategy	ds1	ds2	ds3	ds4	ds5	ds6	ds7	$\bar{x}$
1	+1.0%	-	-	-	-	+2.0%	+9.0%	**+4.0%**
1.1	+3.2%	-	-	-	-	+0.8%	+10.5%	**+4.8%**
2	+4.4%	-	-	-	-	+4.1%	+9.5%	**+6.0%**
2.1	+1.2%	-	-	-	-	+1.6%	+2.9%	**+1.9%**

4. Setting border to limit localization zone: $[0, \bar{dist}_{ek} + \Delta_2]$, where Δ_2 is a tolerance. In this work $\Delta_2 = 5\%$.

5. Identification of neighbours, which are not in the localization zone.

6. Elimination of outliners if their number, n, satisfies the condition: $n \in [0, k/2]$. Otherwise, the algorithm exits. The result of the algorithm is the last evaluation of the position.

7. Position update: calculation of the average coordinates of the remaining neighbors.

For the second modification this work investigates both options: with unstable k (modification 2 when the number of removed neighbors n is replenished by the next neighbors from the distance matrix d) and stable k (modification 2.1).

5.2 Selected numerical results

First and foremost, the proposed strategies were tested against the baseline – in other words, against a basic k-NN with a random choice of one of the three fingerprints taken for one location. Meanwhile, the strategies themselves were also used without preprocessing, meaning the data was selected by random choice as well. The results of testing strategies without preprocessing against the baseline are listed in Table 5.1. As seen, the average gain in accuracy achieves a maximum of 6% for Strategy 2. The rest of the versions turned out to be less successful: 4.8%, 4%, and 1.9% of the average increase in accuracy for strategies 1, 1.1, and 2.1, respectively.

To estimate the general gain from the modifications proposed in this work, it is necessary to compare the strategies against the baseline using preprocessing, i.e., averaging redundancy reduction, which has proven to be the most effective (see Chapter 4). The results for this round of calculations summarized in Table 5.2 show that Strategy 2 remains the most successful, with which it was possible to achieve an improvement in localization quality by 17.2% on average across all datasets, while for datasets 1 and 5 this number exceeds 25%. Among the datasets, the accuracy improvement exceeds 13%

for all of them except ds2 and ds3 - two underground datasets with non-local placement of the GWs.

Table 5.2 Relative Advantages of proposed strategies with preprocessing over the baseline

Strategy	**ds1**	**ds2**	**ds3**	**ds4**	**ds5**	**ds6**	**ds7**	$\bar{x}$
1	+25.2%	+7.3%	+6.0%	+19.0%	+23.5%	+15.1%	+21.6%	**+16.8%**
1.1	+25.2%	+7.3%	+5.7%	+19.0%	+24.2%	+12.2%	+21.5%	**+16.4%**
2	+25.9%	+7.3%	+10.3%	+19.0%	+25.6%	+13.4%	+19.1%	**+17.2%**
2.1	+15.9%	+4.2%	+5.3%	+19.0%	+25.6%	+13.4%	+21.6%	**+15.0%**
$\bar{y}$	**+23.1%**	**+6.5%**	**+6.8%**	**+19.0%**	**+24.7%**	**+13.5%**	**+21.0%**	-

Analyzing the obtained charts, it can be concluded that by using a simple technique to reduce redundancy in combination with the proposed algorithms, it is possible to increase the accuracy of LoRaWAN localization noticeably (up to 17.2% at average).

5.3 Chapter conclusions

This Chapter was focused on investigating the **RQ3**, specifically, how it is algorithmically possible to increase the accuracy of LoRaWAN-based localization. The following conclusions can be drawn from this chapter and oyr related research:

- Among the proposed **accuracy-increasing strategies**, i.e., reassessment from the origin (strategies 1 (Δ = 30%) and 1.1 (Δ = 50%)) and reassessment from the estimated value (strategies 2 (not stable k) and 2.1 (stable k)), the second strategy considering k/3 with changing k turned out to be the most successful one: using the preprocessing it ensures average increase in accuracy of 17.2%.
- Among the **datasets**, the highest error reduction is observed for ds1 (indoor), ds7 (outdoor), ds4, and ds5 (underground), while for the rest, this number is more than 6%.

Despite the accuracy improving techniques proposed in this chapter, the LoRaWAN-based localization still cannot compete with the leading technologies. Nonetheless, the technology could still be applicable in certain scenarios. Specifically, it might be useful in sectors like logistics, agriculture, or smart factories, where LoRaWAN is already in use as a communication method and where high precision in localization is not critical.

Chapter 6

Thesis Conclusions

6.1 Research findings and contributions outline

For this work, three research questions were established, through the prism of which I would like to summarize the obtained results and contributions briefly.

RQ1: Investigation of the metrics and functions of wearable devices that assist enterprises in improving workplace safety levels.

Beginning with an exploration of the field of industrial wearables through a SLR [5], this work has conducted an in-depth examination of the metrics and functions of wearable devices aimed at aiding enterprises in improving workplace safety. As a result the research synthesized two classifications: one on the functions outlined in Table 2.1, and another on the metrics demonstrated in Tables 2.2 and 2.3, respectively.

RQ2: Determining the critical parameters of LoRaWAN from the perspective of localization when planning a measurement campaign and processing its results

Two chapters addressed this issue, and a comprehensive investigation was conducted from the practical perspectives. It was decided to organize several measurement campaigns using different environments (indoor, outdoor, underground). In summary, the qualitative and quantitative outcomes made during the research regarding the investigated parameters, affecting the accuracy of LoRaWAN-based localization, were recaped. From the point of view of the measurement campaign:

- **Environment**: Under ceteris paribus conditions, out of all cases studied, the highest accuracy is observed for the indoor environment ($\sim$ 3 m), followed by the outdoor ($\sim$ 4–5 m) and underground ($\sim$ 6–12 m).
- **Spreading Factor**: The work concludes that employing higher Spreading Factors ensures enhanced localization accuracy by providing a more stable and reliable signal.

From the point of view of data processing:

- **Redundancy Reduction Strategy**: It turned out that the choice of strategy significantly affects the localization accuracy: the random selection of fingerprints is notably less effective (by 12% on average) than the other two, between which the averaging method slightly surpasses the strategy of selecting the maximum RSSI fingerprint.

- **Localization approach**: The methods depending on the position of the GWs, i.e., Trilateration and WCA, were deemed inadequate, resulting in errors between 27-32 m. However, it turned out that applying the ML algorithms can significantly reduce those numbers. A comparative analysis revealed the basic k-NN method ensures the higher accuracy.

The investigation of this question resulted in several contributions. First and foremost, there are open LoRaWAN datasets collected for different environments. Those datasets could benefit a wide array of stakeholders, from researchers exploring the technology to industry leaders optimizing network deployments. Other less significant but nevertheless valuable contributions are mean accuracy error claimed for LoRaWAN-based localization for different environments.

RQ3: Evaluating the potential for enhancing the accuracy of LoRaWAN-based localization through the optimization of localization algorithm.

Within the framework of the last research question, I took into account the results of the comparison of localization approaches, which pointed out the k-NN as the most effective one, and proposed two modifications, based on this method, which are targeted at more successful excluding outliers from the number of neighbors when estimating position. The first strategy employs reassessment from the origin (strategies 1 (Δ = 30%) and 1.1 (Δ = 50%)), while the second one – reassessment from the estimated value (strategies 2 (variable k) and 2.1 (constant k)). Comparing them, it was found that the latter approach of using k/3 with a variable k was the most effective. This strategy, when combined with preprocessing (averaging redundancy reduction strategy), secured an average accuracy improvement of 17.2% compared to the baseline k-NN version and reached up to 92.2% and 90.7% compared to trilateration and WCA, respectively. Although the proposed algorithms are being tested just on the LoRaWAN datasets, they might contribute to any other use case dealing with the k-NN approach.

Thus, with the highest recorded accuracies of $\sim$ 2.6 m indoors and $\sim$ 4 m outdoors, this work posits that LoRaWAN-based localization is feasible for both environments under specific conditions [112]. Although the accuracy-enhancing techniques developed in this research do not allow LoRaWAN-based localization to compare with the leading precision technologies, the idea remains viable for specific scenarios. Particularly, it shows promise in sectors like logistics, agriculture, or smart factories, where LoRaWAN is already used for communication and where extreme precision in localization is not crucial.

6.2 List of original publications

1. **Conference**: Svertoka, E., Rusu-Casandra, A. and Marghescu, I., 2020. "State-of-the-Art of Industrial Wearables: A Systematic Review". In Proc. of 13th International Conference on Communications (COMM) (pp. 411-415). IEEE (**WOS:000612723900073**).

2. **Journal**: Svertoka, E., Bălănescu, M., Suciu, G., Pasat, A. and Drosu, A., 2020. "Decision Support Algorithm Based on the Concentrations of Air Pollutants Visualization". Sensors, 20(20), p.5931 (**Q2, JIF: 3.9, WOS:000585663900001**).

3. **Journal**: Ometov, A., et al., 2021. "A Survey on Wearable Technology: History, State-of-the-Art and Current Challenges". Computer Networks, 193, p.108074 (**Q1, JIF: 5.6, WOS:000774738600002**).

4. **Journal**: Svertoka, E., Saafi, S., Rusu-Casandra, A., Burget, R., Marghescu, I., Hosek, J. and Ometov, A., 2021. "Wearables for Industrial Work Safety: A sSurvey". Sensors, 21(11), p.3844 (**Q2, JIF: 3.9, WOS:000660663600001**).

5. **Journal**: Masek, P., Stusek, M., Svertoka, et al., 2021. "Measurements of LoRaWAN Technology in Urban Scenarios: A Data Descriptor". Data, 6(6), p.62 (**JIF: 2.6, WOS:000665561400001**).

6. **Conference**: Svertoka, E., Marghescu, I., Rusu-Casandra, A., Burget, R., Hosek, J., Masek, P. and Ometov, A., 2022. "Evaluation of Real-Life LoRaWAN Localization: Accuracy Dependencies Analysis Based on Uutdoor Measurement Datasets". In Proc. of 14th International Conference on Communications (COMM) (pp. 1-7). IEEE.

7. **Journal**: Svertoka, E., Rusu-Casandra, A., Burget, R., Marghescu, I., Hosek, J. and Ometov, A., 2022. "LoRaWAN: Lost for localization?". IEEE Sensors Journal, 22(23), pp.23307-23319 (**Q2, JIF: 4.3, WOS:000893571900102**).

6.3 Perspectives for further developments

Returning to the work done, it has opened many directions that could be the subject of interest for future work. Among these directions, it is possible to highlight the refinement of simulation parameters to account for the indoor environment in the HTZ Communication environment and test other propagation models to find the one that most accurately reflects the real picture. It would also be interesting to investigate other underground datasets to confirm the hypothesis about the inapplicability of the technology in underground workspaces. Nevertheless, I consider my work on researching the applicability of LoRaWAN for localization purposes to be complete.

References

[1] International Labor Organization, "World Statistics." Available online: https://www.ilo.org/moscow/areas-of-work/occupational-safety-and-health/WCMS_249278/lang--en/index.htm (accessed on Tuesday 9th April, 2024).

[2] S. Ketu and P. K. Mishra, "Internet of healthcare things: A contemporary survey," *Journal of Network and Computer Applications*, vol. 192, p. 103179, 2021.

[3] IoT Business News, "State of IoT 2022." Available online: https://iotbusinessnews.com/2022/05/19/70343-state-of-iot-2022-number-of-connected-iot-devices-growing-18-to-14-4-billion-globally/#:~:text=supply (accessed on Tuesday 9th April, 2024).

[4] A. Ometov, S. V. Bezzateev, J. Kannisto, J. Harju, S. Andreev, and Y. Koucheryavy, "Facilitating the Delegation of Use for Private Devices in the Era of the Internet of Wearable Things," *IEEE Internet of Things Journal*, vol. 4, no. 4, pp. 843–854, 2016.

[5] E. Svertoka, S. Saafi, A. Rusu-Casandra, R. Burget, I. Marghescu, J. Hosek, and A. Ometov, "Wearables for industrial work safety: A survey," *Sensors*, vol. 21, no. 11, p. 3844, 2021.

[6] A. Hinze, J. Bowen, and J. L. König, "Wearable technology for hazardous remote environments: Smart shirt and rugged iot network for forestry worker health," *Smart Health*, vol. 23, p. 100225, 2022.

[7] J. Khakurel, H. Melkas, and J. Porras, "Tapping into the Wearable Device Revolution in the Work Environment: A Systematic Review," *Information Technology & People*, 2018.

[8] Optalert, "Eagle Industrial." Available online: https://www.optalert.com/explore-products/eagle-industrial/ (accessed on Tuesday 9th April, 2024).

[9] Qoowear, "Boosting The Safety Of Workers In Sub-Zero Environments." Available online: http://qoowear.com/ (accessed on Tuesday 9th April, 2024).

[10] Eleksen, "Smart Workforce Safety." Available online: https://eleksen.com/ (accessed on Tuesday 9th April, 2024).

[11] MyExposome, "Lightweight Simple Wristbands." Available online: http://www.myexposome.com/approach (accessed on Tuesday 9th April, 2024).

[12] Laevo Exoskeletons, "Our Wearable Chest and Back Support." Available online: https://www.laevo-exoskeletons.com/en/laevo-v2 (accessed on Tuesday 9th April, 2024).

[13] DIGI, "Kinetic Creates An Innovative Wearable That Reduces Workplace Injuries And Increases Safety Using Digi IoT Solutions." Available online: https://www.digi.com/customer-stories/kinetic-wearable-reduces-workplace-injuries (accessed on Tuesday 9th April, 2024).

[14] J. Masood, A. Dacal-Nieto, V. Alonso-Ramos, M. I. Fontano, A. Voilqué, and J. Bou, "Industrial Wearable Exoskeletons and Exosuits Assessment Process," in *Proc. of International Symposium on Wearable Robotics*, pp. 234–238, Springer, 2018.

[15] Codered, "Signal 21 Speaker Microphone." Available online: https://www.coderedheadsets.com/Signal-21-Speaker-Microphone-p/signal21.htm (accessed on Tuesday 9th April, 2024).

[16] Spectro:o, "Spectro:o Digital Signage Platform." Available online: https://spectroo.eu/?lang=en (accessed on Tuesday 9th April, 2024).

[17] Realwear, "RealWear – Digital Workflow with Industrial Wearable." Available online: https://www.gitex.com/video-gallery/realwear-digital-workflow-with-industrial-wearable (accessed on Tuesday 9th April, 2024).

[18] Capgemini, "Augmented and Virtual Reality." Available online: https://www.capgemini.com/wp-content/uploads/2018/09/AR-VR-in-Operations1.pdf (accessed on Tuesday 9th April, 2024).

[19] Solepower, "Powering The Future One Step At A Time." Available online: http://www.solepowertech.com/#solepower (accessed on Tuesday 9th April, 2024).

[20] M. Santos, S. Vollam, M. A. Pimentel, C. Areia, L. Young, C. Roman, J. Ede, P. Piper, E. King, M. Harford, *et al.*, "The use of wearable pulse oximeters in the prompt detection of hypoxemia and during movement: diagnostic accuracy study," *Journal of Medical Internet Research*, vol. 24, no. 2, p. e28890, 2022.

[21] Y. Fu and J. Liu, "System design for wearable blood oxygen saturation and pulse measurement device," *Procedia manufacturing*, vol. 3, pp. 1187–1194, 2015.

[22] CardioMedive, "CardioMedive." Available online: https://cardiomedive.eu/?ref=fab-romania#/ (accessed on Tuesday 9th April, 2024).

[23] WebMDe, "Diastole vs. Systole: Know Your Blood Pressure Numbers." Available online: https://www.webmd.com/hypertension-high-blood-pressure/guide/diastolic-and-systolic-blood-pressure-know-your-numbers#1 (accessed on Tuesday 9th April, 2024).

[24] Fourier, "Blood Pressure Sensor DT098." Available online: https://fourieredu.com/fwp/store/products/blood-pressure-sensor (accessed on Tuesday 9th April, 2024).

[25] Vernier, "Blood Pressure Sensor." Available online: https://www.vernier.com/product/blood-pressure-sensor/ (accessed on Tuesday 9th April, 2024).

[26] G. S. Stergiou, B. Alpert, S. Mieke, R. Asmar, N. Atkins, S. Eckert, G. Frick, B. Friedman, T. Graßl, T. Ichikawa, *et al.*, "A Universal Standard for the Validation of Blood Pressure Measuring Devices: Association for the Advancement of Medical Instrumentation/European Society of Hypertension/International Organization

for Standardization (AAMI/ESH/ISO) Collaboration Statement," *Hypertension*, vol. 71, no. 3, pp. 368–374, 2018.

[27] A. Pantelopoulos and N. G. Bourbakis, "A Survey on Wearable Sensor-Based Systems for Health Monitoring and Prognosis," *IEEE Transactions on Systems, Man, and Cybernetics, Part C (Applications and Reviews)*, vol. 40, no. 1, pp. 1–12, 2009.

[28] D. M. Bard, J. I. Joseph, and N. van Helmond, "Cuff-less Methods for Blood Pressure Telemonitoring," *Frontiers in Cardiovascular Medicine*, vol. 6, p. 40, 2019.

[29] F. Fotouhi-Ghazvini and S. Abbaspour, "Wearable Sireless Sensors for Measuring Calorie Consumption," *Journal of Medical Signals and Sensors*, vol. 10, no. 1, p. 19, 2020.

[30] J. Lester, C. Hartung, L. Pina, R. Libby, G. Borriello, and G. Duncan, "Validated Caloric Expenditure Estimation Using a Single Body-worn Sensor," in *Proc. of 11th International Conference on Ubiquitous Computing*, pp. 225–234, 2009.

[31] S. K. Jain and B. Bhaumik, "An Energy Efficient ECG Signal Processor Detecting Cardiovascular Diseases on Smartphone," *IEEE Transactions on Biomedical Circuits and Systems*, vol. 11, no. 2, pp. 314–323, 2016.

[32] D. Azariadi, V. Tsoutsouras, S. Xydis, and D. Soudris, "ECG Signal Analysis and Arrhythmia Detection on IoT Wearable Medical Devices," in *Proc. of 5th International Conference on Modern Circuits and Systems Technologies (MOCAST)*, pp. 1–4, IEEE, 2016.

[33] M. Li, W. Xiong, and Y. Li, "Wearable measurement of ecg signals based on smart clothing," *International Journal of Telemedicine and Applications*, vol. 2020, 2020.

[34] QARDIO, "QARDIOCORE." Available online: https://www.getqardio.com/qardiocore-wearable-ecg-ekg-monitor-iphone/ (accessed on Tuesday 9th April, 2024).

[35] Y. Athavale and S. Krishnan, "Biosignal Monitoring Using Wearables: Observations and Opportunities," *Biomedical Signal Processing and Control*, vol. 38, pp. 22–33, 2017.

[36] D. P. Subha, P. K. Joseph, R. Acharya, and C. M. Lim, "EEG Signal Analysis: A Survey," *Journal of Medical Systems*, vol. 34, no. 2, pp. 195–212, 2010.

[37] Y. Wei, Y. Wu, and J. Tudor, "A Real-time Wearable Emotion Detection Headband based on EEG Measurement," *Sensors and Actuators A: Physical*, vol. 263, pp. 614–621, 2017.

[38] J. W. Ahn, Y. Ku, and H. C. Kim, "A Novel Wearable EEG and ECG Recording System for Stress Assessment," *Sensors*, vol. 19, no. 9, p. 1991, 2019.

[39] Emotiv, "Brain Controlled Technology." Available online: https://www.emotiv.com/brain-controlled-technology/ (accessed on Tuesday 9th April, 2024).

[40] C. Hettiarachchi, J. Kodithuwakku, B. Manamperi, A. Ifham, and P. Silva, "A Wearable System to Analyze the Human Arm for Predicting Injuries due to Throwing," in *Proc. of 41st Annual International Conference of the IEEE Engineering in Medicine and Biology Society (EMBC)*, pp. 3297–3301, IEEE, 2019.

[41] Papakostas, Michalis and Kanal, Varun and Abujelala, Maher and Tsiakas, Konstantinos and Makedon, Fillia, "Physical fatigue detection through EMG wearables and subjective user reports: a machine learning approach towards adaptive rehabilitation," in *Proceedings of the 12th ACM International Conference on PErvasive Technologies Related to Assistive Environments*, pp. 475–481, 2019.

[42] B. Milosevic, S. Benatti, and E. Farella, "Design challenges for wearable emg applications," in *Design, Automation & Test in Europe Conference & Exhibition (DATE), 2017*, pp. 1432–1437, IEEE, 2017.

[43] Shimmer, "Shimmer3 EMG Unit." Available online: https://www.emotiv.com/brain-controlled-technology/ (accessed on Tuesday 9th April, 2024).

[44] Myonetic, "Sports." Available online: https://www.myontec.com/sports (accessed on Tuesday 9th April, 2024).

[45] J. He, W. Choi, X. Wu, and Y. Yang, "Detection of operator drowsiness using google glass," in *Proceedings of the Human Factors and Ergonomics Society Annual Meeting*, vol. 59, pp. 1607–1611, SAGE Publications Sage CA: Los Angeles, CA, 2015.

[46] W.-J. Chang, L.-B. Chen, and Y.-Z. Chiou, "Design and implementation of a drowsiness-fatigue-detection system based on wearable smart glasses to increase road safety," *IEEE Transactions on Consumer Electronics*, vol. 64, no. 4, pp. 461–469, 2018.

[47] MedlinePlus, "Diabetes." Available online: https://medlineplus.gov/ency/article/001214.htm (accessed on Tuesday 9th April, 2024).

[48] P. S. Ciechanowski, W. J. Katon, J. E. Russo, and I. B. Hirsch, "The Relationship of Depressive Symptoms to Symptom Reporting, Self-Care and Glucose Control in Diabetes," *General Hospital Psychiatry*, vol. 25, no. 4, pp. 246–252, 2003.

[49] D. Rodin, M. Kirby, N. Sedogin, Y. Shapiro, A. Pinhasov, and A. Kreinin, "Comparative Accuracy of Optical Sensor-based Wearable System for Non-invasive Measurement of Blood Glucose Concentration," *Clinical Biochemistry*, vol. 65, pp. 15–20, 2019.

[50] WHOOP, "Overview of the Whoop Strap 3.0." Available online: https://www.whoop.com/thelocker/whoop-strap-3-0-overview/ (accessed on Tuesday 9th April, 2024).

[51] T. Bobrowski and W. Schuhmann, "Long-Term Implantable Glucose Biosensors," *Current Opinion in Electrochemistry*, vol. 10, pp. 112–119, 2018.

[52] D. Meetoo, L. Wong, and B. Ochieng, "Smart Tattoo: Technology for Monitoring Blood Glucose in the Future," *British Journal of Nursing*, vol. 28, no. 2, pp. 110–115, 2019.

[53] B. Bellmann, C. Gemein, and P. Schauerte, "Regular Pulse Rate but Irregular Heart Rate?," *Netherlands Heart Journal*, vol. 24, no. 6, pp. 435–437, 2016.

[54] Z. Ge, P. Prasad, N. Costadopoulos, A. Alsadoon, A. Singh, and A. Elchouemi, "Evaluating the Accuracy of Wearable Heart Rate Monitors," in *Proc. of 2nd International Conference on Advances in Computing, Communication, & Automation (ICACCA)(Fall)*, pp. 1–6, IEEE, 2016.

[55] C. Hanning and J. Alexander-Williams, "Fortnightly Review: Pulse Oximetry: A Practical Review," *Bmj*, vol. 311, no. 7001, pp. 367–370, 1995.

[56] Myzone, "MZ-3." Available online: https://www.myzone.org/mz-3 (accessed on Tuesday 9th April, 2024).

[57] A. K. Dwivedi, S. A. Imtiaz, and E. Rodriguez-Villegas, "Algorithms for Automatic Analysis and Classification of Heart Sounds–A Systematic Review," *IEEE Access*, vol. 7, pp. 8316–8345, 2018.

[58] C. Wong, Z.-Q. Zhang, B. Lo, and G.-Z. Yang, "Wearable Sensing for Solid Biomechanics: A Review," *IEEE Sensors Journal*, vol. 15, no. 5, pp. 2747–2760, 2015.

[59] A. Ometov, D. Solomitckii, T. Olsson, S. Bezzateev, A. Shchesniak, S. Andreev, J. Harju, and Y. Koucheryavy, "Secure and Connected Wearable Intelligence for Content Delivery at a Mass Event: A Case Study," *Journal of Sensor and Actuator Networks*, vol. 6, no. 2, p. 5, 2017.

[60] M. Norris, R. Anderson, and I. C. Kenny, "Method Analysis of Accelerometers and Gyroscopes in Running Gait: A Systematic Review," *Proc. of the Institution of Mechanical Engineers, Part P: Journal of Sports Engineering and Technology*, vol. 228, no. 1, pp. 3–15, 2014.

[61] M. Webster, "Sweat." Available online: https://www.merriam-webster.com/dictionary/sweat (accessed on Tuesday 9th April, 2024).

[62] C. Legner, U. Kalwa, V. Patel, A. Chesmore, and S. Pandey, "Sweat Sensing in the Smart Wearables Ara: Towards Integrative, Multifunctional and Body-Compliant Perspiration Analysis," *Sensors and Actuators A: Physical*, vol. 296, pp. 200–221, 2019.

[63] M. Parrilla, T. Guinovart, J. Ferré, P. Blondeau, and F. J. Andrade, "A Wearable Paper-based Sweat Sensor for Human Perspiration Monitoring," *Advanced Healthcare Materials*, vol. 8, no. 16, p. 1900342, 2019.

[64] MyHealthyApple.com, "Top Four Sweat Sensor Telated Features Coming Soon to Your Smartwatches." Available online: https://www.myhealthyapple.com/top-four-sweat-sensors-related-features-coming-soon-to-your-smartwatch/#What_are_sweat_sensors (accessed on Tuesday 9th April, 2024).

[65] The free dictionary, "Respiration Rate." Available online: https://medical-dictionary.thefreedictionary.com/respiration+rate (accessed on Tuesday 9th April, 2024).

[66] R. De Fazio, M. Stabile, M. De Vittorio, R. Velázquez, and P. Visconti, "An overview of wearable piezoresistive and inertial sensors for respiration rate monitoring," *Electronics*, vol. 10, no. 17, p. 2178, 2021.

[67] I. I. Geneva, B. Cuzzo, T. Fazili, and W. Javaid, "Normal Body Temperature: A Systematic Review," in *Open Forum Infectious Diseases*, vol. 6, p. ofz032, Oxford University Press US, 2019.

[68] F. MacDonald, "This is How a Norwegian Woman Survived the Lowest Body Temperature Ever Recorded." Available online: https://www.sciencealert.com/this-woman-survived-the-lowest-body-temperature-ever-recorded (accessed on Tuesday 9th April, 2024).

[69] Thermometrics, "Accuracy Standards." Available online: https://www.thermometricscorp.com/rtd-accuracy.html (accessed on Tuesday 9th April, 2024).

[70] Maxim Integrated, "Max30205 Human Body Temperature Sensor." Available online: https://www.maximintegrated.com/en/products/interface/sensor-interface/MAX30205.html (accessed on Tuesday 9th April, 2024).

[71] Workerbase, "First Smartwatch for Industrial Use." Available online: https://workerbase.com/industrial-smartwatch (accessed on Tuesday 9th April, 2024).

[72] Z. Mohy-Ud-Din, S. H. Woo, J. H. Lee, S. H. Lee, P. S. Young, C. H. Won, and J. H. Cho, "Wireless skin temperature sensing patch," in *2008 IEEE International Conference on Multisensor Fusion and Integration for Intelligent Systems*, pp. 258–260, IEEE, 2008.

[73] E. Svertoka, M. Bălănescu, G. Suciu, A. Pasat, and A. Drosu, "Decision support algorithm based on the concentrations of air pollutants visualization," *Sensors*, vol. 20, no. 20, p. 5931, 2020.

[74] E. Svertoka, A. Rusu-Casandra, and I. Marghescu, "State-of-the-art of industrial wearables: A systematic review," in *Proc. of 13th International Conference on Communications (COMM)*, pp. 411–415, IEEE, 2020.

[75] Cambridge Dictionary, "Atmospheric pressure." Available online: https://dictionary.cambridge.org/ru (accessed on Tuesday 9th April, 2024).

[76] Alex Yartsev. Deranged Physiology, "Physiological Effects of High and Low Barometric Pressure." Available online: https://derangedphysiology.com/main/cicm-primary-exam/required-reading/respiratory-system/Chapter%20923/physiological-effects-high-and-low-barometric-pressure (accessed on Tuesday 9th April, 2024).

[77] Y. Melamed, A. Shupak, and H. Bitterman, "Medical problems associated with underwater diving," *New England Journal of Medicine*, vol. 326, no. 1, pp. 30–35, 1992.

[78] Vandrico Inc, "Atheer Air Glasses." Available online: https://vandrico.com/wearables/device/atheer-air-glasses.html (accessed on Tuesday 9th April, 2024).

[79] Maximum Yield, "Light Intensity." Available online: https://www.maximumyield.com/definition/2036/light-intensity (accessed on Tuesday 9th April, 2024).

[80] National Optical Astronomic Observatory, "Recommended Light Levels." Available online: http://www.noao.edu/education/QLTkit/ACTIVITY_Documents/Safety/LightLevels_outdoor+indoor.pdf (accessed on Tuesday 9th April, 2024).

[81] European Commission. Health and Consumers. Scientific Committees, "Health Effects of Artificial Light." Available online: https://ec.europa.eu/health/scientific_committees/opinions_layman/artificial-light/en/l-2/4-effects-health.htm#0 (accessed on Tuesday 9th April, 2024).

[82] E. E. K. Nang, G. Abuduxike, P. Posadzki, U. Divakar, N. Visvalingam, N. Nazeha, G. Dunleavy, G. I. Christopoulos, C.-K. Soh, K. Jarbrink, *et al.*, "Review of the Potential Health Effects of Light and Environmental Exposures in Underground Workplaces," *Tunnelling and Underground Space Technology*, vol. 84, pp. 201–209, 2019.

[83] United States Department of Labor. Occupational Safety and Health Administration., "Standard 1926.56 – Illumination." Available online: https://www.osha.gov/laws-regs/regulations/standardnumber/1926/1926.56 (accessed on Tuesday 9th April, 2024).

[84] M. Mardonova and Y. Choi, "Review of Wearable Device Technology and Its Applications to the Mining Industry," *Energies*, vol. 11, no. 3, p. 547, 2018.

[85] Texas Instruments, "OPT3006 Ultra-Thin Ambient Light Sensor." Available online: https://www.ti.com/product/OPT3006 (accessed on Tuesday 9th April, 2024).

[86] The Free Dictionary, "Noise level." Available online: https://www.thefreedictionary.com/noise+level (accessed on Tuesday 9th April, 2024).

[87] M. Talukdar, "Noise Pollution and its Control in Textile Industry," 2001.

[88] Cambridge Dictionary, "Radiation." Available online: https://dictionary.cambridge.org/ru (accessed on Tuesday 9th April, 2024).

[89] U.S.NRC, "Information for Radiation Workers." Available online: https://www.nrc.gov/about-nrc/radiation/health-effects/info.html (accessed on Tuesday 9th April, 2024).

[90] EPA. United States Environmental Protection Agency, "Radiation Health Effects." Available online: https://www.epa.gov/radiation/radiation-health-effects (accessed on Tuesday 9th April, 2024).

[91] A. Banafa, "The internet of everything," 04 2014.

[92] Cambridge Dictionary, "Relative Humidity." Available online: https://dictionary.cambridge.org/ru (accessed on Tuesday 9th April, 2024).

[93] J. Toftum and P. O. Fanger, "Air Humidity Requirements for Human Comfort," *ASHRAE transactions*, vol. 105, p. 641, 1999.

[94] A. Baughman and E. A. Arens, "Indoor Humidity and Human Health–Part I: Literature Review of Health Effects of Humidity-Influenced Indoor Pollutants," *ASHRAE Transactions*, vol. 102, pp. 192–211, 1996.

[95] Sensirion, "Datasheet sht1x (sht10, sht11, sht15) Humidity and Temperature Sensor." Available online: https://www.sparkfun.com/datasheets/Sensors/SHT1x_datasheet.pdf (accessed on Tuesday 9th April, 2024).

[96] M. A. Milley and G. B. O'Keefe, "Mountain Warfare and Cold Weather Operations," tech. rep., Headquarters Department of the Army Washington United States, 2016.

[97] W. Cui, G. Cao, J. H. Park, Q. Ouyang, and Y. Zhu, "Influence of Indoor Air Temperature on Human Thermal Comfort, Motivation and Performance," *Building and Environment*, vol. 68, pp. 114–122, 2013.

[98] World Health Organization, "Radiation: The Ultraviolet (UV) Index." Available online: https://www.who.int/news-room/q-a-detail/radiation-the-ultraviolet-(uv)-index (accessed on Tuesday 9th April, 2024).

[99] K. Vanicek, T. Frei, Z. Litynska, and A. Schmalwieser, "UV-Index for the Public," *Publication of the European Communities, Brussels, Belgium*, 2000.

[100] S. Banerjee, E. G. Hoch, P. D. Kaplan, and E. L. Dumont, "A Comparative Study of Wearable Ultraviolet Radiometers," in *Proc. of IEEE Life Sciences Conference (LSC)*, pp. 9–12, IEEE, 2017.

[101] Vantage Market Research, "LPWAN market." Available online: https://www.vantagemarketresearch.com/industry-report/low-power-wide-area-network-market-1127#:~:text=Global (accessed on Tuesday 9th April, 2024).

[102] A. Augustin, J. Yi, T. Clausen, and W. M. Townsley, "A study of lora: Long range & low power networks for the internet of things," *Sensors*, vol. 16, no. 9, p. 1466, 2016.

[103] Y. Singh, "Comparison of okumura, hata and cost-231 models on the basis of path loss and signal strength," *International journal of computer applications*, vol. 59, no. 11, 2012.

[104] "New SID on NR-Lite for Industrial Sensors and Wearables," TDoc RP-191048, 3GPP, June 2019.

[105] ETSI, "3GPP TR 36.873 V12.7.0 (2017-12)." Available online: https://portal.3gpp.org/desktopmodules/Specifications/SpecificationDetails.aspx?specificationId=2574 (accessed on Tuesday 9th April, 2024).

[106] Adeunis, "FTD: network tester ." Available online: https://www.adeunis.com/en/produit/ftd-network-tester/#zone-dl (accessed on Tuesday 9th April, 2024).

[107] M. Gineprini, S. Parrino, G. Peruzzi, and A. Pozzebon, "Lorawan performances for underground to aboveground data transmission," in *2020 IEEE international instrumentation and measurement technology conference (I2MTC)*, pp. 1–6, IEEE, 2020.

[108] G. Di Renzone, S. Parrino, G. Peruzzi, A. Pozzebon, and D. Bertoni, "Lorawan underground to aboveground data transmission performances for different soil compositions," *IEEE Transactions on Instrumentation and Measurement*, vol. 70, pp. 1–13, 2021.

[109] C. Ebi, F. Schaltegger, A. Rüst, and F. Blumensaat, "Synchronous lora mesh network to monitor processes in underground infrastructure," *IEEE access*, vol. 7, pp. 57663–57677, 2019.

[110] S. Wilson and R. Laing, "Wearable technologies: Present and future," in *91st World Conference of The Textile Institute. Leeds, UK*, 2018.

[111] E. Svertoka, I. Marghescu, A. Rusu-Casandra, R. Burget, J. Hosek, P. Masek, and A. Ometov, "Evaluation of real-life lorawan localization: Accuracy dependencies analysis based on outdoor measurement datasets," in *2022 14th International Conference on Communications (COMM)*, pp. 1–7, IEEE, 2022.

[112] E. Svertoka, A. Rusu-Casandra, R. Burget, I. Marghescu, J. Hosek, and A. Ometov, "Lorawan: Lost for localization?," *IEEE Sensors Journal*, vol. 22, no. 23, pp. 23307–23319, 2022.